# Transcriptional Characterization of Neuronal Cell Populations in Prairie Voles

**Conor J. Kelly**
Molecular, Cellular, and Developmental Biology
University of Colorado at Boulder

**Defense Date:**
April 2, 2018

**Thesis Advisor:**
Zoe Donaldson, Molecular, Cellular, and Developmental Biology & Psychology and Neuroscience

**Defense Committee:**
Dr. Zoe Donaldson, Molecular, Cellular, and Developmental Biology & Psychology and Neuroscience
Dr. David Root, Psychology and Neuroscience
Dr. Jennifer Martin, Molecular, Cellular, and Developmental Biology

## Abstract

As humans, we experience the profound biological necessity to form social bonds from the moment of birth. These bonds are imperative for normal development and impact our health and well-being, with strong social networks acting as a primary predictor of longevity. The lack of or disruption of such bonds can be debilitating, as shown by increased rates of mental and physical illnesses. Our understanding of social bonds has been limited because commonly used laboratory model organisms, such as rats and mice, do not form partner-specific social bonds. To study complex social behaviors, the monogamous rodent, the prairie vole (*M. ochrogaster*), has provided a valuable model as they form life-long pair bonds. Studies looking at hormonal and peptidergic regulation of pair bonding have identified candidate genes in the formation and maintenance of pair bonds, but little is known about the global transcriptional changes that accompany pair bond formation. Here, I pioneer in voles translating ribosome affinity purification (TRAP) with the aim of purifying actively translating mRNA from genetically defined cell types within the nucleus accumbens. I show that the TRAP transgene is highly expressed in a Cre recombinase-dependent manner. Further optimizations are required in order to obtain more highly intact actively translating mRNAs. We propose combining TRAP with an activity dependent labeling system in voles, allowing for the isolation of actively translating mRNA in cells active during mating and evidence for the first time of the global changes in transcription that accompany pair bond formation.

## Introduction

As humans, we experience the profound biological necessity to form social bonds from the moment of birth. These bonds are imperative for normal development and impact our health and well-being, with strong social networks acting as a primary predictor of longevity[1-4]. The lack of or disruption of such bonds can be debilitating, as shown by increased rates of mental and physical illnesses[5-7]. Given the universality and importance of social bonds, there is a pressing need to identify the neurogenetic mechanisms that contribute to bonding.

Prairie voles (*Microtus ochrogaster*) have been studied because they form partner-specific bonds and exhibit behaviors associated with monogamy. The traits most commonly used to characterize monogamy include the following: (a) the formation of a preference to interact and mate with a particular individual, or pair bond; (b) male and female cohabitation throughout breeding and non-breeding seasons; (c) biparental care, including high levels of paternal care; and (d) aggression toward unrelated conspecifics[8-9]. The biological basis of these traits has been difficult to study in part because commonly used laboratory model organisms, such as rats and mice, do not exhibit these traits. Although the monogamous prairie vole has provided a valuable model to study complex social behaviors, our understanding of the mechanisms underlying these behaviors could be improved through the implementation of neurogenetic tools that are well established in mice and rats.

### Prairie Voles – a Model for Monogamy

Among the 3-5% of mammals that pair bond[8], the prairie vole has arisen as an excellent model organism for monogamy in rodents. Initial observations during ecological studies suggested that prairie voles might be monogamous because the same two individuals were repeatedly caught in

traps in the wild[10]. Subsequent laboratory studies using the partner preference test, in which a subject can freely spend its time with a familiar mating partner, a novel individual, or in isolation in a "neutral" zone, revealed that prairie voles are monogamous, as subjects spent more time huddling with their partners than interacting with the novel individual[11]. Because they form selective social preferences and exhibit behaviors characteristic of monogamy, prairie voles constitute a valuable mammalian model for studying human social behaviors[12-14]. Prairie voles rarely take a new partner in the wild after the death of a previous partner, suggesting that these preferences are enduring[15]. Interestingly, closely-related microtine species such as the montane (*M. montanus*) and meadow (*M. pennsylvanicus*) vole are sexually promiscuous, do not develop mating-induced partner preferences, and do not exhibit selective aggression or biparental care[10, 16-17]. The genetic and molecular mechanisms underlying these species-specific differences in social behavior are largely unclear.

Previous studies have demonstrated that pair bonding results in substantial, enduring changes in behavior that are not observed in non-bonded individuals. Additionally, studies looking at hormonal and peptidergic regulation of pair bonding have identified candidate genes that modulate these behavioral changes upon bond formation in prairie voles[18-24]. In particular, coordinated signaling of both oxytocin and dopamine in the NAcc is required for pair bonding, suggesting the NAcc may integrate sociocognitive and reward-related information during attachment[23]. However, to my knowledge, there have been no attempts to characterize the global transcriptional changes to elucidate the mechanisms by which pair bonding induces these enduring changes in behavior. The purpose of my thesis is to develop novel techniques in voles to isolate mRNA from neurons in the NAcc.

**Transcriptional Characterization of Activity-Dependent Neuronal Ensembles**

Current research suggests that the enduring shift in behavior that accompanies pair bonding is the result of transcriptional changes in a subset of candidate genes. Sexually naïve prairie voles find social novelty rewarding, whereas pair bonded voles will avoid and act aggressively towards novel conspecifics[25]. This observation led Resendez and colleagues to hypothesize that this pair bond-dependent shift in behavior is accompanied by the upregulation of neural systems that regulate selective aggression in prairie voles (i.e. D1-like receptor and dynorphin/KOR systems)[26]. Dynorphin and D1-like receptor mRNA transcript levels isolated from cells within the NAcc shell were elevated in bonded prairie voles relative to sibling-housed prairie voles, and subsequent blocking of D1-like receptors diminished selective aggression in bonded prairie voles[26,27]. These findings indicate that selective aggression is modulated, at least in part, by an upregulation in D1-like receptor mRNA and activity.

Arginine vasopressin 1a receptor (V1aR) signaling is also crucial for modulating the onset of selective aggression following pair bonding. In bonded male prairie voles, the onset of selective aggression occurs as a result of increased expression of V1aR mRNA in the anterior hypothalamus following bond formation[28]. Overexpression of V1aR using AAVs into the anterior hypothalamus of sexually naïve males induced aggression towards novel females, whereas administration of V1aR antagonists into the same region diminished selective aggression in bonded males[28]. These studies provide striking evidence that the pair bond-induced behavioral changes result from changes in expression of a select subset of candidate genes coding for signaling molecules necessary for pair bond formation and maintenance. However, global transcriptional changes in defined neuronal subpopulations remain unexplored. Therefore,

I adapted and implemented technologies that allow for the examination of the transcriptional changes underlying pair bond formation within specific neuronal subpopulations.

In order to characterize relevant transcriptional plasticity that may underlie pair bonding, the mRNA of defined neurons must be isolated. Adult mammalian brain tissue is highly heterogeneous, containing hundreds of distinct and densely interwoven neuronal and glial cell types. Isolation of one particular subtype from a tissue composed of many different cell types is challenging, requiring ways to identify neuronal types based on genetic identity, projection patterns, or activity. For my thesis, I will isolate mRNA from genetically defined neurons in the NAcc to resolve the issue of heterogeneity that has thus far complicated transcriptional studies in prairie voles.

The goal of my thesis is to pioneer in voles two systems – translating ribosomal affinity purification (TRAP, Fig. 1)[29,30] and fluorescence-activated cell sorting (FACS) – to isolate mRNA from specific neuronal populations in the NAcc of prairie voles. To achieve this, I will isolate RNA from neurons within the NAcc using a neuron-specific promoter. This will provide the groundwork for future studies identifying the cellular basis underlying the enduring changes in behavior that accompany pair bond formation.

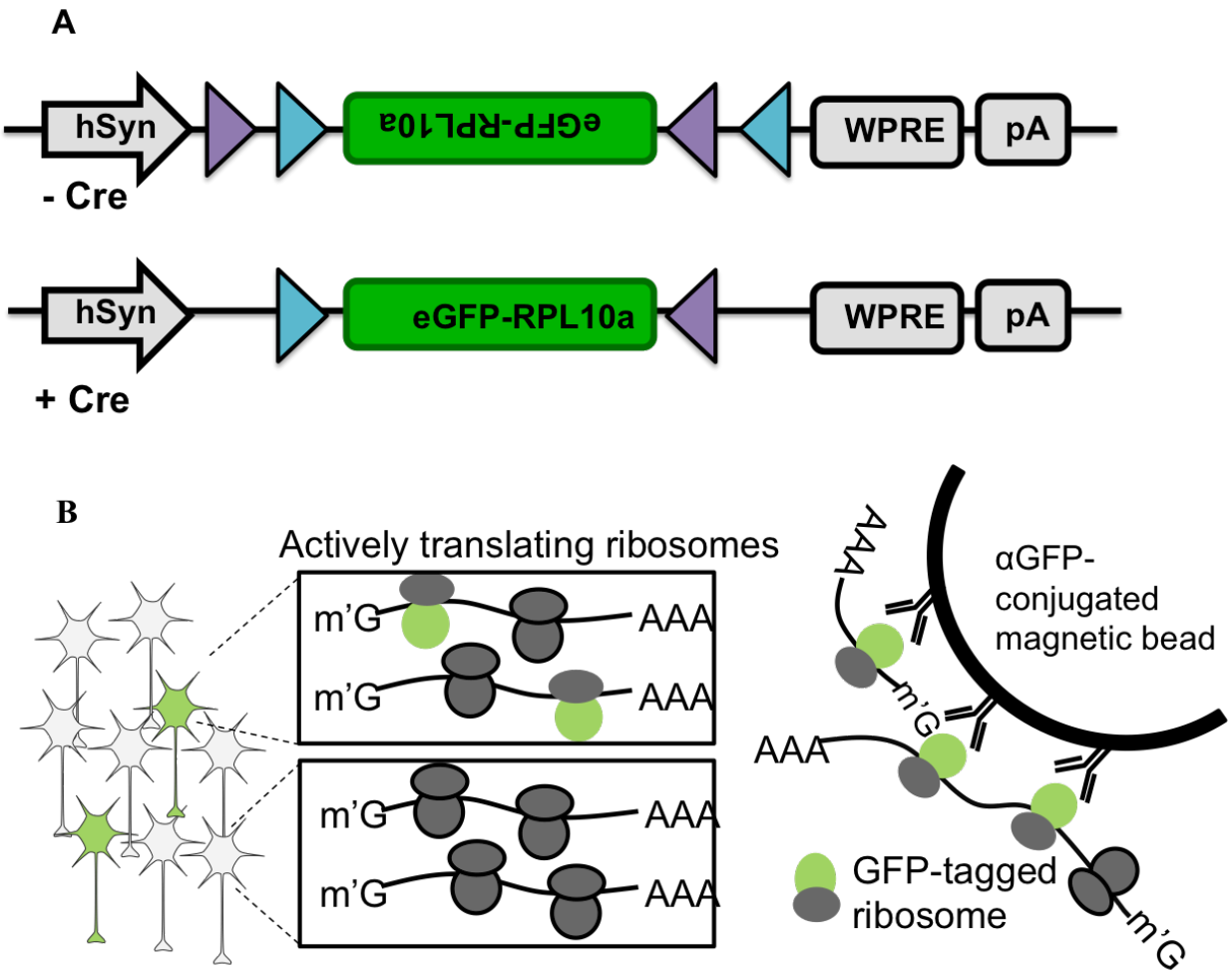


**Figure 1.** pAAV-hSyn-DIO-eGFP-RPL10a allows for eGFP-labeling of the 60S ribosomal protein L10a (RPL10a). A) TRAP utilizes an affinity tag, such as enhanced green fluorescent protein (eGFP), fused to the large ribosomal subunit protein L10a[29,30]. Cell-type specificity is accomplished by driving expression of the transgene using the neuron-specific human synapsin (hSyn) promoter[37]. The eGFP-RPL10a coding sequence (green) is floxed by a pair of loxP (blue) and lox2272 (purple) sites. In the absence of Cre recombinase, the eGFP-RPL10a coding sequence is inverted relative to the hSyn promoter. When expressed, Cre recombinase inverts the eGFP-RPL10a sequence into an active orientation by "flipping" and then "locking" the lox2272 and loxP sites. B) Neurons expressing the eGFP-RPL10a fusion protein will incorporate the eGFP-labeled RPL10a protein into the ribosomes over time. Monoclonal antibodies specific for eGFP are used to immunoprecipitate eGFP-tagged ribosomes and attached mRNA, after which the eGFP-tagged ribosomes are washed away. This results in a pool of actively translating mRNAs isolated from a genetically defined neuronal population.

# Methods

## Plasmid Cloning and Packaging

*Generating pAAV-hSyn-DIO-eGFPpvRPL10a*

To generate the TRAP construct, the DNA fragment containing the vole RPL10a sequence was inserted into the pAAV-hSyn-DIO-eGFP (Addgene plasmid #50457) backbone. The RPL10a fragment was designed for cloning using the NEBuilder HiFi Assembly method and consisted of a 5' homology arm sequence, a linker sequence coding for SGRTQISSSSFEF, the vole RPL10a sequence (GenBank XM_005360358.1), and a 3' homology arm sequence (Supplementary Fig. 1). pAAV-hSyn-DIO-eGFP was digested using restriction endonucleases Asc1 (NEB) and BsrG1-HF (NEB), and the linearized plasmid was purified using the Zymogen Gel DNA Recovery Kit. The cloned plasmid, hereafter referred to as pAAV-hSyn-DIO-eGFPpvRPL10a, was generated using the NEBuilder HiFi DNA Assembly Cloning kit and subsequently transfected into 5-alpha F'$I^q$ Competent *E. coli* (NEB). Transfected bacteria were selected for using carbenicillin (100ug/ml) and harvested using the EZDNA Plasmid Mini Kit (Omega) or HiSpeed Plasmid Maxi Kit (Qiagen). The sequence of pAAV-hSyn-DIO-eGFPpvRPL10a was verified using Sanger sequencing (QuintaraBio) and restriction digest (Supplementary Table 1, Supplementary Fig. 2) before being sent for viral packaging (Stanford Neuroscience Gene Vector and Virus Core).

*Preparation and confirmation of pAAV-RAM-d2tTA-TRE-iCre*

pAAV-RAM-d2tTA-TRE-iCre (courtesy of Yinxi Lin) was used to transfect 5-alpha F'$I^q$ Competent *E. coli* (NEB). Transfected bacteria were selected for using ampicillin and harvested using EZNA Plasmid Mini Kit (Omega) or HiSpeed Plasmid Maxi Kit (Qiagen).

The sequence of pAAV-RAM-d2tTA-TRE-iCre was verified using Sanger sequencing (QuintaraBio) and restriction digest (Supplementary Table 1, Supplementary Fig. 3) before being sent for viral packaging (Stanford Neuroscience Gene Vector and Virus Core).

**Prairie Vole Subjects**

Prairie voles used in this study were laboratory-reared animals derived from two established colonies at the University of California Davis (courtesy of Karen Bales) and Emory University (courtesy of Larry Young). To enhance genetic diversity, we established our colony by breeding voles from these two distinct backgrounds together. Adult female and male prairie voles were 7-10 weeks of age for all surgeries. Following stereotaxic viral vector injections, voles were housed with up to three same-sex adult individuals in a temperature- and humidity-controlled room on a 12 hr light/dark schedule (lights on at 7:00 AM/lights off at 7:00 PM) and provided with food and water *ad libitum*. All prairie vole protocols were performed in accordance with NIH standard ethical guidelines and were approved by the Institutional Animal Care and Use Committee (IACUC) at the University of Colorado Boulder (protocol #2435).

**Viral Injection, Microdissections, and Perfusions**

Adult prairie voles were anesthetized using isoflurane (3% induction, 1-2.5% maintenance) and secured to a stereotactic frame (Kopf) with a heating pad to maintain body temperature. Animals were injected sub-dermally with Meloxicam SR (Zoopharm, 4.0mg/kg) and sterile saline (Nurse Assist). Using a glass pipette connected to a Nanoject II (Drummond Scientific) injector, AAVs were delivered to the brain and allowed to diffuse for 10 min before withdrawing the pipette. The coordinates of the target brain structures in reference to bregma (mm) were as followed: nucleus

accumbens shell (AP: -1.7, ML: ±1.0, DV: -4.7, -4.6, -4.5, -4.4, -4.3 or -4.7, -4.5, -4.3) and medial amygdala (AP: -1.25, ML: +2.5, DV: -6.2, -6.0, -5.8, -5.6). The skin was sealed with vicryl sutures (eSutures), after which the animals were given topical antibiotic ointment (Globe Scientific). Voles were allowed to recover in their homecage for a minimum of 13 days prior to tissue harvesting. For microdissections, the prairie voles were rapidly decapitated, and the nucleus accumbens tissue of both hemispheres was dissected out by hand in less than 5 minutes. Animals used for fluorescent confocal imaging received a lethal injection of 0.2ml 1:2 ketamine/xylazine and were perfused with 1X phosphate buffer saline (PBS) followed by 4% paraformaldehyde in 1X PBS. Perfused brains were placed in 1ml of 4% paraformaldehyde for 24 hours, after which they were transferred to 5ml of 30% sucrose and allowed to sink prior to sectioning.

**Fluorescent Confocal Imaging**

Perfused brains were mounted onto a microtome (Leica JungSM2000R) using OCT (Fisher Healthcare) and frozen with dry ice. 50um sections were prepared from each brain and stored in 24-well plates (Falcon) containing 1ml of 1X PBS and 0.05% sodium azide (Thermo Fisher). Sections were mounted onto Superfrost Plus glass slides (Thermo Fisher), treated with 200ul of ProLong Diamond Antifade Mountant (Invitrogen), and covered with cover slips (Globe Scientific). After sitting at room temperature for 24 hours, prepared slides were sealed with nailpolish (Electron Microscopy Sciences). Prepared slides were imaged using an Olympus IX81 Inverted Widefield Microscope and a Yokogawa CV1000 Confocal Scanner System (University of Colorado Light Microscopy Core Facility). Stitched images were produced using ImageJ 1.51n[31].

**Verification of TRAP Expression**

To validate expression of virally introduced pAAV-hSyn-DIO-eGFPpvRPL10a, male prairie voles (n=2) received unilateral injections into the right NAcc with 450nl (150nl/site, 1nl/sec) of a viral cocktail containing 1.5ul AAV8-hSyn-Cre-mCherry (5.9E12 vg/ml, UNC) and 3ul of AAV1-DIO-eGFP-RPL10a (2.22E12 vg/ml). The animals were allowed to recover for 18 days in their homecage prior to perfusion.

To determine if expression of eGFP-RPL10a is Cre recombinase-dependent, adult male prairie voles (n=2) received unilateral injections into the right NAcc with 450nl (150nl/site, 1nl/sec) of a viral cocktail containing 2ul of AAV1-hSyn-DIO-eGFPpvRPL10a (2.22E12 vg/ml) and 2ul of AAV2-hSyn-mCherry (4.70E12 vg/ml, UNC) in 4ul cortex buffer. The animals were allowed to recover for 13 days in their homecage prior to perfusion.

**TRAP and RNA Extraction**

Adult female prairie voles (n=3) received bilateral injections into the NAcc with 500nl (100nl/site, 1nl/sec) per hemisphere of a viral cocktail containing 2ul of AAV1-hSyn-DIO-eGFPpvRPL10a (2.22E12 vg/ml), 2ul of AAV1-hSyn-iCre (1.56E13 vg/ml, SigmaGen SL101441), and 4ul cortex buffer. Injected voles were allowed to recover for eight weeks, after which they were rapidly decapitated and both hemispheres of nucleus accumbens tissue were dissected using a 1mm coronal hamster brain matrix (Zivic Instruments) and processed according to a protocol published by Heiman and colleagues[30] (summarized below). The affinity matrices were prepared using 300ul of 10 mg/ml Streptavidin MyOne T1 Dynabeads (Invitrogen), 150ul of 1ug/ul Biotinylated Protein L (Fisher Scientific), and 50ug each of eGFP antibodies Htz-19C8 and Htz-19F7 (Memorial-Sloan Kettering Monoclonal Antibody Facility). Two groups of tissue

were processed in parallel: one containing tissue from two animals for a total of four hemispheres and another containing tissue from one animal for a total of two hemispheres. Dissected tissue was placed in dissection buffer (1X HBSS, 2.5mM HEPES, 35mM glucose, 4mM $NaHCO_3$, 100ug/ul cycloheximide) and homogenized using a rotor homogenizer in 1ml of lysis buffer (20mM HEPES, 150mM KCl, 10mM $MgCl_2$, 0.5mM DTT, 100ug/ul cycloheximide, 10ul/ml Rnasin, 10ul/ml Superasin) about 5 minutes after the dissection, taking care to keep the homogenizer nozzle fully submerged to avoid introducing bubbles. Homogenates were centrifuged (10 min, 2,000g), and the resulting post-nuclear supernatant was treated with 1% NP-40 (AG Scientific) and 30 mM DHPC (Avanti Polar Lipids) and centrifuged (10 min, 20,000g). 1ml of the resulting post-mitochondrial supernatant was added to the prepared affinity matrices and allowed to incubate at 4°C for 24 hours. The remaining ~150ul of post-mitochondrial supernatant was flash frozen in dry ice and stored at −80°C as input for RNA extraction the following day. After 24 hours, the unbound fraction was removed as flowthrough and stored on wet ice for same-day RNA extraction, and the beads were washed four times with 1ml of high salt buffer (20mM HEPES, 150mM KCl, 10mM $MgCl_2$, 10% NP-40, RNase-free water, protease inhibitor tablets, 0.5mM DTT, 100ug/ul cycloheximide). The RNA was washed from the anti-eGFP bound ribosomes using 300ul of SKP buffer from the Norgen RNA/DNA Purification Kit, 3.0ul b-mercaptoethanol (Amresco), 1.0ul of recombinant RNAsin (Promega), and 1.0ul of Superasin (Applied Biosystems). The RNA of the pulldown, input, and flowthrough samples was purified using the Norgen RNA/DNA Purification Kit according to the manufacturer's instructions. The RNA was eluted from the columns twice using two volumes of 13ul Elution Solution A (Norgen). Eluted RNA was stored at −80°C.

**Preparation of TRAP cDNA**

2ul of each thawed TRAP RNA sample was submitted to the BioFrontiers Institute Next-Gen Sequencing Core Facility for QC analysis using an Agilent 2100 Bioanalzyer with pico chip. The input and flowthrough RNA samples were diluted 1:3 prior to QC analysis. The resulting concentration measurements were used to standardize the concentration of the RNA used to make cDNA. RNA samples within groups were standardized based on the concentration of the lowest concentration sample in that group. 40ul of cDNA was prepared from each sample using the High Capacity cDNA Reverse Transcription Kit (Applied Biosystems) as instructed by the manufacturer. The resulting cDNA was then stored at -20°C.

**Single Cell Suspension Preparation for FACS**

A cohort of adult female prairie voles (n=11) received bilateral intracranial injections into the nucleus accumbens using 450nl per hemisphere (150nl per site, 1nl/sec) of a viral cocktail containing 1ul of AAV8-hSyn-eGFP (4.2E12 vg/ml) and 14ul cortex buffer per hemisphere at a rate of 1nl/sec. The injected voles were allowed eighteen days to recover in their homecage, when they were rapidly decapitated. Both hemispheres of nucleus accumbens tissue were dissected out and transferred to a sterile 1.5ml microcentrifuge tube, flash frozen on dry ice, and stored at −80°C for several months. To obtain a single cell suspension, either one or both hemispheres were removed from −80°C and processed according to a protocol published by Rubio and colleagues[32]. Briefly, tissue was minced on ice and added to 1ml Hibernate A Low Fluorescence buffer (BrainBits) and centrifuged (2 min, 110g at 4°C). 1ml of Accutase (Thermo Fisher Scientific) was added to the resulting pellet. After a 30 minute incubation at 4°C, the samples were centrifuged (2 min, 960g at 4°C), and the supernatant was discarded. 1.0ml of Hibernate A Low Fluorescence buffer was added to each sample. The samples were then

triturated using glass pipettes of decreasing diameter (1.3mm, 0.8mm, 0.4mm) and fixed using either 50% ethanol or 4% paraformaldehyde. Fixed cells were centrifuged (4 min, 1,700g at 4°C), washed with 1X PBS, and strained using 100um and 50um cell strainers (BD Falcon). Processed cell suspensions were manually counted using a hemocytometer and inverted epifluorescent microscope (Leica DM IL LED) and imaged using an Olympus IX81 Inverted Widefield Microscope (University of Colorado Light Microscopy Core Facility).

**Verification of RAM**

Female prairie voles (n=9) were co-injected into the left medial amygdala using 128nl (32nl/site, 1nl/sec) viral cocktail containing 1ul of AAV2/5-RAM-mKate, 1ul of AAV1-hSyn-eGFP, and 8ul of cortex buffer. Animals were returned to their homecage and maintained on DOX chow for 7 days, after which they were switched to regular chow. 36 hours later, experimental animals received an opposite sex vole, whereas homecage controls had their cage lid removed and the experimenter placed a hand in the cage. Animals were perfused 24 hours later.

## Results

*Validation of pAAV-hSyn-DIO-eGFPpvRPL10a Expression*

I first compared the nucleotide and amino acid sequences for RPL10a in mice and prairie voles. The mouse RPL10a cDNA sequence was input into BLASTX 2.8.0[33], and the resulting protein alignment against the prairie vole RPL10a amino acid sequence was 100% identical with an E-value of $3\times10^{-145}$ (Fig. 2). To assess nucleotide homology, the mouse RPL10a cDNA sequence was aligned to the vole RPL10a cDNA sequence using BLASTN 2.8.0[33] with a percent identity of 93% and an E-value of 0.0 (Fig. 3). Although the amino acid sequences are identical between mice and prairie voles, I generated pAAV-hSyn-DIO-eGFPpvRPL10a using the prairie vole RPL10a cDNA sequence to account for any possible species-specific differences in aminoacyl-tRNA concentrations.

To validate expression of virally introduced pAAV-hSyn-DIO-eGFPpvRPL10a, male prairie voles (n=2) received unilateral injections into the NAcc using a viral cocktail containing AAV8-hSyn-Cre-mCherry and AAV1-DIO-eGFPpvRPL10a. There is striking overlap cells dual positive for mCherry and eGFP, indicating successful transfection and expression of the Cre-mCherry and eGFP-RPL10a constructs (Fig. 4). To determine if expression of eGFP-RPL10a is indeed Cre recombinase-dependent, female prairie voles (n=2) received unilateral injections into the NAcc with a viral cocktail containing AAV1-hSyn-DIO-eGFPpvRPL10a and AAV2-hSyn-mCherry. As expected, all cells observed were positive for mCherry but not eGFP (Fig. 5). Together, these findings indicate that pAAV-hSyn-DIO-eGFPpvRPL10a, when introduced into the NAcc shell virally, is expressed strongly but only in the presence of Cre recombinase.

```
Mouse       10 MSSKVSRDTLYEAVREVLHGNQRKRRKFLETVELQISLKNYDPQKDKRFSGTVRLKSTPR
Vole         1 MSSKVSRDTLYEAVREVLHGNQRKRRKFLETVELQISLKNYDPQKDKRFSGTVRLKSTPR
consensus      ************************************************************

Mouse       61 PKFSVCVLGDQQHCDEAKAVDIPHMDIEALKKLNKNKKLVKKLAKKYDAFLASESLIKQI
Vole       190 PKFSVCVLGDQQHCDEAKAVDIPHMDIEALKKLNKNKKLVKKLAKKYDAFLASESLIKQI
consensus      ************************************************************

Mouse      370 PRILGPGLNKAGKFPSLLTHNENMVAKVDEVKSTIKFQMKKVLCLAVAVGHVKMTDDELV
Vole       121 PRILGPGLNKAGKFPSLLTHNENMVAKVDEVKSTIKFQMKKVLCLAVAVGHVKMTDDELV
consensus      ************************************************************

Mouse      550 YNIHLAVNFLVSLLKKNWQNVRALYIKSTMGKPQRLY
Vole       181 YNIHLAVNFLVSLLKKNWQNVRALYIKSTMGKPQRLY
consensus      ***********************************
```

**Figure 2**. Alignment of mouse (*M. musculus*) and prairie vole (*M. ochrogaster*) ribosomal protein L10a (RPL10a) amino acid sequences. The mouse RPL10a amino acid sequence was deduced from the mouse RPL10a cDNA sequence (GenBank BC083346.1) and aligned to the prairie vole RPL10a amino acid sequence (XP_005360415.1) using BLASTX 2.8.0+[33]. Asterisks indicate matching amino acids. The mouse and vole amino acid sequences are 100% identical, with an expected value of 3E-145.

```
Mouse       5   CAGCCATGAGCAGCAAAGTCTCACGCGACACCCTGTACGAGGCGGTGCGGGAAGTCCTGC
Vole        53  CAGCCATGAGCAGCAAAGTCTCTCGCGACACCCTGTACGAGGCGGTGCGGGAGGTCCTGC
consensus       ********************** ***************************** *******

Mouse       113 ACGGGAACCAGCGCAAGCGCCGCAAGTTTCTGGAGACGGTGGAGCTGCAGATCAGCCTGA
Vole        65  ACGGGAACCAGCGCAAGCGCCGCAAGTTTCTGGAAACGGTGGAGCTGCAGATCAGCCTGA
consensus       ********************************** ************************

Mouse       125 AGAACTACGACCCTCAGAAGGACAAACGTTTCTCGGGCACCGTCAGGCTCAAGTCCACCC
Vole        173 AGAACTACGACCCCCAGAAGGACAAGCGTTTCTCGGGCACCGTCAGGCTCAAGTCCACCC
consensus       ************* *********** ***********************************

Mouse       185 CACGCCCCAAGTTCTCGGTGTGCGTTCTGGGGGACCAGCAGCACTGTGATGAAGCCAAGG
Vole        233 CTCGCCCCAAGTTCTCAGTGTGTGTCCTGGGGGACCAGCAGCACTGCGATGAGGCCAAGG
consensus       * ************** ***** ** ******************** ***** *******

Mouse       245 CCGTGGATATCCCCCACATGGACATCGAGGCGCTCAAGAAGCTTAACAAAAACAAGAAGT
Vole        293 CCGTGGATATCCCCCACATGGACATCGAGGCGCTGAAGAAGCTCAATAAGAACAAGAAGT
consensus       ********************************** ******** ** ** **********

Mouse       305 TGGTCAAGAAGCTGGCTAAGAAGTACGATGCCTTTTTGGCCTCTGAGTCTCTGATTAAGC
Vole        353 TGGTCAAAAAGCTGGCCAAGAAGTATGACGCCTTTCTGGCCTCTGAGTCTCTGATCAAGC
consensus       ******* ******** ******** ** ****** ****************** ****

Mouse       365 AGATCCCACGTATCCTGGGCCCAGGCCTAAACAAGGCTGGCAAGTTCCCCTCCCTGCTGA
Vole        413 AGATCCCGCGTATCCTGGGCCCAGGCCTGAACAAGGCTGGCAAGTTCCCTTCCCTGCTGA
consensus       ******* ******************** ******************** **********

Mouse       425 CACACAATGAAAACATGGTGGCCAAAGTGGATGAGGTGAAATCGACAATCAAGTTCCAGA
Vole        473 CACACAATGAAAACATGGTGGCCAAAGTGGACGAGGTGAAGTCCACGATCAAGTTCCAGA
consensus       ******************************** ******** ** ** *************

Mouse       485 TGAAGAAGGTGCTGTGTTTGGCCGTCGCTGTTGGCCACGTGAAGATGACCGATGATGAGC
Vole        533 TGAAGAAGGTGCTGTGTCTGGCTGTCGCTGTCGGCCACGTGAAGATGACCGACGACGAGC
consensus       ***************** **** ******** ******************** ** ****

Mouse       545 TAGTCTACAACATTCATCTGGCTGTCAATTTCTTGGTGTCCTTGCTTAAGAAAAACTGGC
Vole        593 TGGTCTACAACATCCACTTGGCTGTCAATTTCTTGGTGTCCTTGCTCAAGAAGAACTGGC
consensus       * ************ **  *************************** *****.*******

Mouse       605 AAAACGTGCGGGCTCTGTACATCAAGAGCACCATGGGCAAGCCCCAGCGTCTGTATTAGG
Vole        653 AAAATGTCCGGGCTTTGTATATCAAGAGCACCATGGGCAAGCCCCAGCGTCTTTACTAGG
consensus       **** ** ****** **** ******************************** ** ****

Mouse       665 ATGCTCCAATAAACCT
Vole        713 ATGCCCCAATAAACCT
consensus       **** ************
```

**Figure 3**. Alignment of mouse (*M. musculus*) and prairie vole (*M. ochrogaster*) ribosomal protein L10a (RPL10a) cDNA sequences. The mouse RPL10a mRNA sequence (GenBank BC083346.1) was aligned to the prairie vole RPL10a cDNA sequence (XP_005360358.1) using BLASTN 2.8.0+[33]. Asterisks indicate matching nucleotides. The mouse and vole cDNA sequences are 93% identical, with an expected value of 0.0.

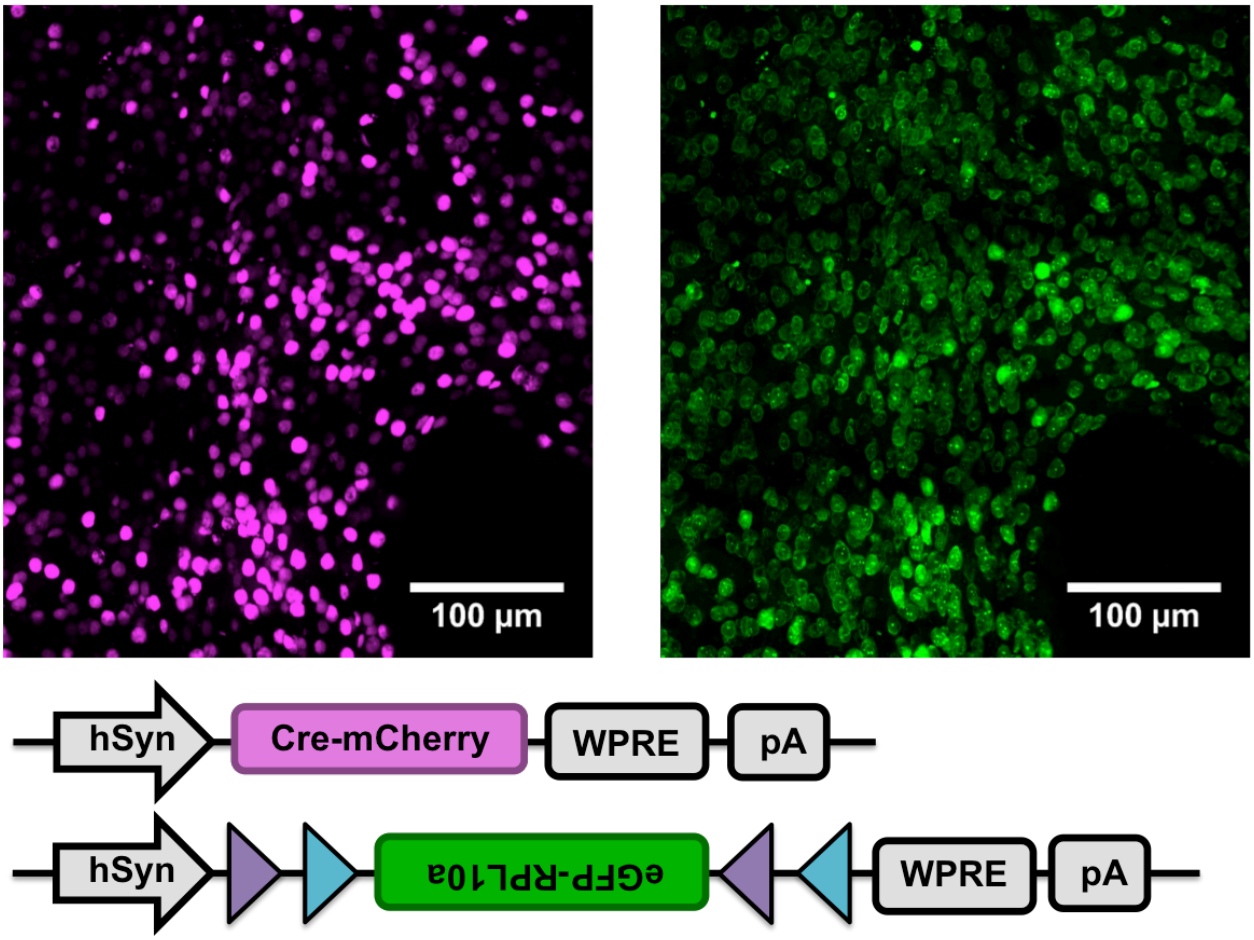


**Figure 4.** Expression of Cre recombinase drives expression of the eGFP-Rpl10a fusion protein. A cohort of male prairie voles (n=2) received unilateral injections into the right NAcc of a viral cocktail containing AAV8-hSyn-Cre-mCherry and AAV1-DIO-eGFP-RPL10a. The injected voles were allowed to recover for 18 days in their homecage prior to perfusion. Left: stitched maximum intensity projection taken in the red channel. Right: stitched maximum intensity projection taken in the green channel. Magenta = cells expressing mCherry, green = cells expressed eGFP-RPL10a. Images were taken at 40X on a Yokogawa CellVoyager CV1000 and stitched using ImageJ 1.51n[31]. Image credit: Julie Sadino.

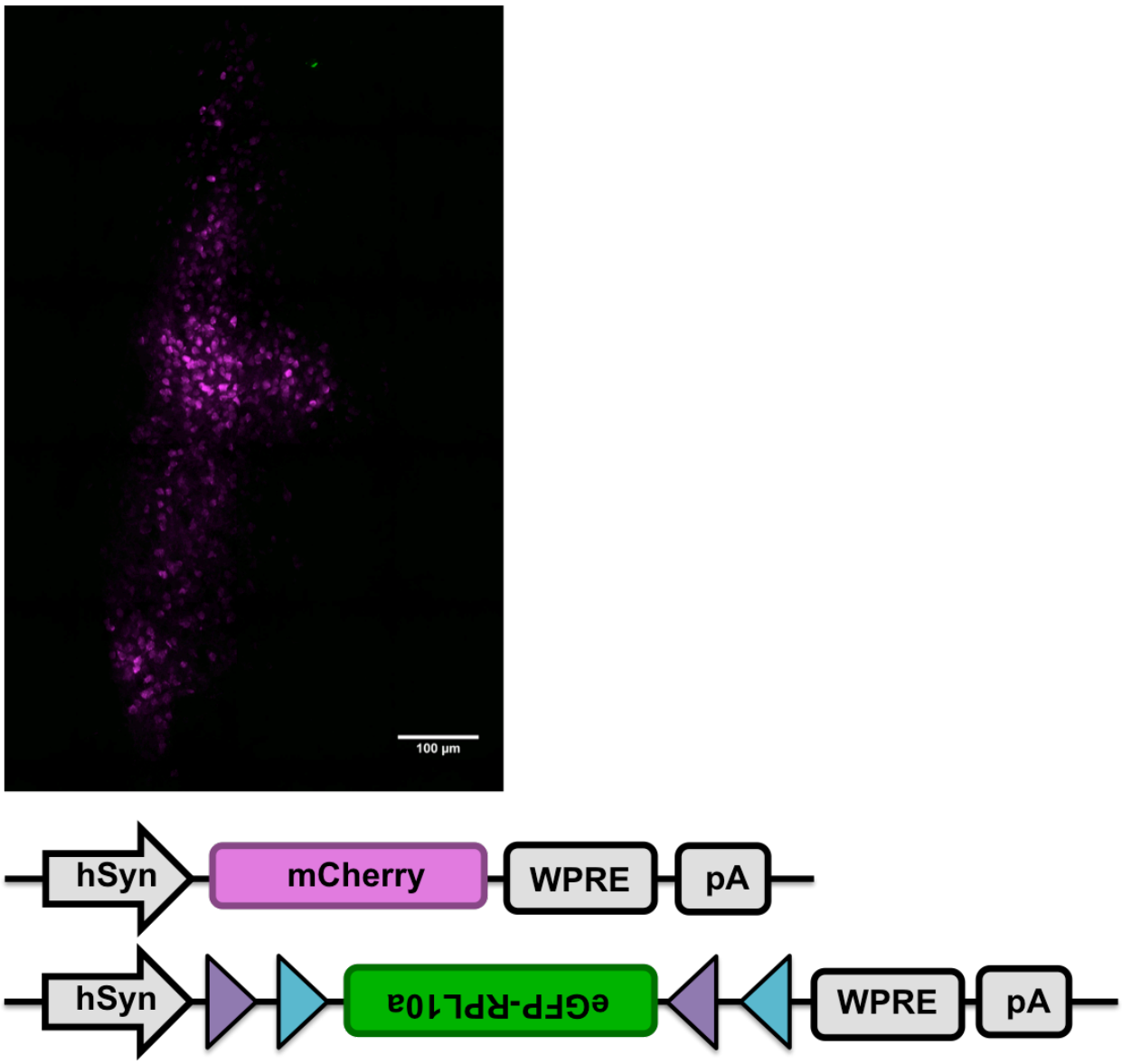


**Figure 5.** Expression of the TRAP transgene is Cre-recombinase dependent. Female prairie voles (n=2) received unilateral injections into the right NAcc of a viral cocktail containing AAV2-hSyn-mCherry and AAV1-DIO-eGFP-RPL10a. The injected voles were allowed to recover for 13 days in their homecage prior to perfusion. The stitched image shown here was generated by merging the maximum intensity projection taken in the red and green channels. Magenta = cells expressing mCherry, green = cells expressed eGFP-RPL10a. Images were taken at 40X on a Yokogawa CellVoyager CV1000 and stitched and merged using ImageJ 1.51n[31].

*Purification of Actively Translating mRNA*

Having determined that expression of the TRAP transgene is Cre-dependent, I sought to evaluate the amount of tissue required to obtain an adequate quantity of actively translating mRNA for downstream analysis using quantitative polymerase chain reaction (qPCR). Female adult prairie voles (n=3) received bilateral injections into the NAcc with AAV1-DIO-eGFPpvRPL10a and AAV1-hSyn-iCre. To assess the amount of tissue required to obtain adequate yield, two TRAP reactions were performed side-by-side: one containing dissected NAcc tissue from both hemispheres of one animal (designated "2H") and another containing NAcc tissue from both hemispheres of two animals ("4H"). Pulldown, input, and flowthrough RNA samples were purified as discussed above (see Methods). The input and flowthrough samples were assigned high RIN values, ranging from 7.7 to 8.1 (Fig. 6, Table 1). As expected, the concentrations of RNA in the input and flowthrough for both samples were relatively high compared to the pulldowns. For each sample, the concentration of the input RNA was greater than the concentration of the flowthrough, and the concentrations of the input and flowthrough RNA from the sample containing four hemispheres of tissue were greater than those from the sample containing two hemispheres (Table 1). However, quality control analysis indicates that the RNA in the pulldown samples was highly degraded, as they were assigned RIN values of "N/A" (Fig. 6A, Table 1). Looking at the electropherograms for these samples, I observed small peaks corresponding to intact 18S and 28S rRNA, although the magnitudes of these peaks are very small as compared to the inputs and flowthroughs (Fig. 6B). Nonetheless, bands corresponding to intact 18S and 28S rRNA are evident, albeit at low intensity (Fig. 6A). The concentrations of RNA in both pulldown samples are lower than expected (Table 1). Curiously, the concentration

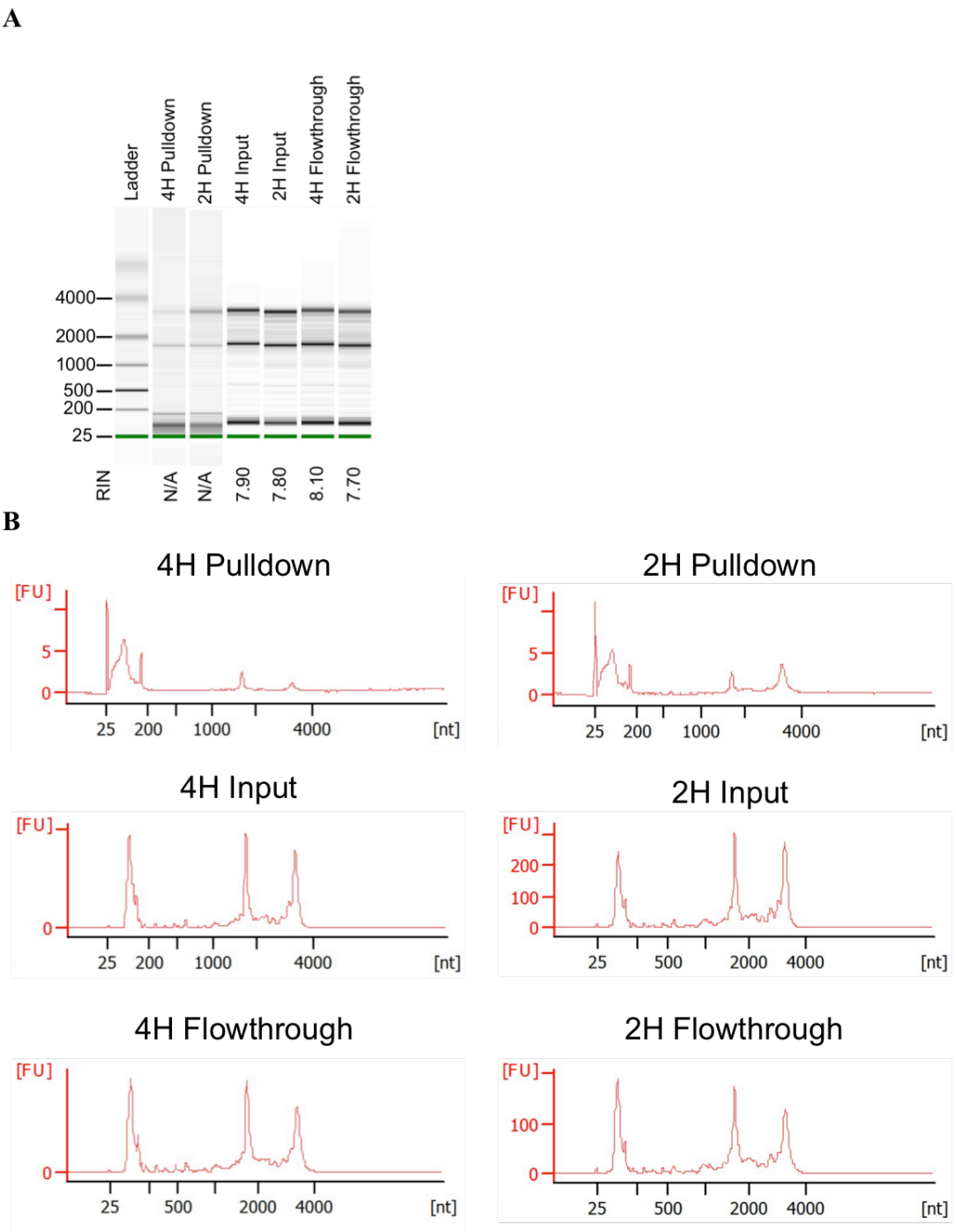


**Figure 6.** Quality control analysis of TRAP RNA. A) The integrity of the TRAP RNA samples was determined using an Agilent 2100 Bioanalyzer with a pico chip. The input and flowthrough RNA samples were diluted 1:3 prior to QC analysis, whereas the pulldown RNA samples were undiluted. Bands of approximately 3500nt correspond to intact 28S rRNA, while bands 1750nt are representative of intact 18S rRNA. B) Electropherograms for each sample were generated from the intensities of the bands in Figure A.

| Sample RNA | | Concentration (ng/ul) | RIN |
|---|---|---|---|
| 4 Hemispheres of NAcc Tissue | Pulldown | 0.322 | N/A |
| | Input | 80.752 | 7.9 |
| | Flowthrough | 74.364 | 8.1 |
| 2 Hemispheres of NAcc Tissue | Pulldown | 0.345 | N/A |
| | Input | 52.228 | 7.8 |
| | Flowthrough | 37.144 | 7.7 |

**Table 1**. Concentrations and RIN values of RNA samples. Two samples were prepared, one containing four hemispheres of NAcc tissue and another containing two hemispheres of NAcc tissue. The pulldown RNA constitutes the RNA that was eluted from the dissociated eGFP-labeled ribosomes. The input RNA was isolated from the post-mitochondrial supernatant. The Flowthrough RNA was isolated from the unbound fraction following the 24 hour incubation.

of RNA in the 4H pulldown sample was less than the concentration of RNA in the 2H pulldown sample.

*Preparation of Single Cell Suspension for FACS Sorting*

While TRAP allows for the purification of the actively translating mRNA content of a group of cells, FACS can be used to isolate to isolate the total RNA content of a single cell. To sort transfected NAcc cells expressing eGFP from cells not expressing eGFP, I attempted to obtain a single cell suspension for input into FACS. A cohort of female prairie voles (n=2) received bilateral injections into the NAcc with AAV8-hSyn-eGFP. A combination of uninjected tissue and tissue injected with AAV8-hSyn-eGFP was dissected and processed, but the resulting cell suspensions were highly clumped and not devoid of debris despite thorough filtration (Fig. 7). Modifications to the protocol may include increasing the length of the accutase incubation and decreasing the internal diameters of the glass pipettes used to triturate the homogenates. Additionally, little fluorescence was observed from processed injected tissue (Fig. 7). I suspected that the 100% ethanol used to fix the cells was quenching the eGFP signal and instead used 4% paraformaldehyde. Nonetheless, very few fluorescing cells were observed. Further optimization is required before we can employ FACS to isolate neurons expressing eGFP.

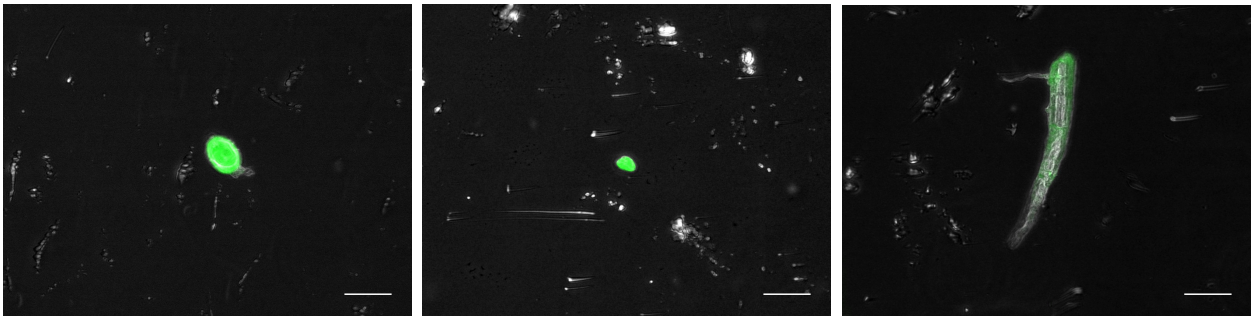

**Figure 7**. Preparation of cell suspensions from virally injected adult vole brain tissue. A cohort of adult female voles (n=2) received bilateral injections into the nucleus accumbens with AAV8-hSyn-eGFP. The resulting cell suspensions had clumps of cells indicating incomplete digestion, and little fluorescence was observed. Images were taken at 20X on an Olympus IX81 Inverted Widefield Microscope. Scale bars = 50um.

## Discussion

Here I demonstrate that TRAP can be modified for use in voles, allowing for the transcriptional characterization of genetically defined cell types within a particular region of the brain. I show that cells virally transfected with the TRAP construct containing the vole RPL10a sequence robustly express the TRAP transgene only in the presence of Cre recombinase. Additionally, I provide evidence that TRAP can be modified in voles to successfully purify eGFP-labeled ribosomes from which actively translating mRNA can be isolated.

Further optimization is required to increase the quality and yield of the pulldown RNA isolated from the affinity matrix. Changes to improve yield include pooling tissue from more injected animals, eluting RNA from the same affinity matrices twice, and eluting the RNA from the extraction column with a lower volume of elution buffer. However, as the pooling size increases, the time required to homogenize those samples, and thus the risk of sample degradation, increases. Previous experiments performed by collaborators have shown that intact RNA can be extracted from tissue that is flash frozen and stored at −80°C, although this may decrease overall yield[30]. Additionally, using a viral approach presents a unique challenge in that it is difficult to confirm whether there is expression of the TRAP transgene in a set of injected tissue for input into TRAP. The fact that the concentration of the pulldown RNA from the 4H sample was lower than that of the 2H sample suggests that at least one of the injections within the 4H group was a miss. Although the pulldown RNA samples were of low integrity, the flowthrough RNA samples were relatively intact, suggesting that more care needs to be taken when washing the affinity matrices. Assuming successful isolation of more highly intact pulldown RNA, this pulldown RNA can be used to make cDNA for qPCR analysis with neuronal and glial specific markers to assess the degree of neuronal specificity of the human synapsin promoter. Despite the need for

optimization, this trial experiment provides evidence for successful implementation of TRAP in prairie voles.

Attempts to produce a single-cell suspension from tissue virally injected with a construct expressing eGFP under the control of the neuron-specific hSyn promoter were largely unsuccessful. The cell suspensions contained clumped cells and cellular debris. Additional filtration steps or the use of density gradients may reduce the concentration of clumps and debris. However, this may introduce more sources of stress and facilitate RNA degradation. Notably, very few fluorescent cells were observed from homogenates prepared from tissue injected with AAV8-hSyn-eGFP. This could result from a faulty viral construct, missed injections, imprecise microdissections, or chemical quenching of fluorescent signal. Previous experiments provided evidence for expression of AAV8-hSyn-eGFP in the NAcc of injected adult voles. Dissected tissue can be quickly observed under an epifluorescent dissecting scope to check for expression prior to flash freezing. Successful preparation of single cell suspensions from tissue virally injected with a construct expressing eGFP and subsequent isolation of eGFP-expressing neurons would allow for input into single-cell RNA-seq, providing a precise method to measure the level of transcripts in a single, particular cell that cannot be accomplished through sequencing techniques such as RNA-seq that uses RNA from pooled cells[34].

According to the neural network hypothesis, understanding how the brain translates transient experience into changes in neural circuits requires the identification of neuronal ensembles, or groups of neurons that show spatiotemporal co-activation, that encode each experience. Unlike the neuron doctrine, which defines the individual neuron as the functional unit of the nervous system, the neural network models argue that the neural circuitry arises from the activation of

neuronal ensembles[34]. In this model, animal behavior is dynamically encoded within networks of activity-dependent neuronal ensembles. Changes in synaptic activity in local networks may serve as the key mechanism to linking neuronal ensembles in a behaviorally relevant fashion[34]. The question becomes, then, how to characterize neuronal ensembles that are active during a specific, temporally defined behavioral paradigm.

My thesis applies TRAP as a method of isolating actively translating mRNA from neurons using a cell-type specific promoter. TRAP is highly versatile in that it can be combined with other tools to isolate neurons according to their projection patterns or activity. To isolate neurons active during a specific behavioral paradigm, we propose combining TRAP with the robust activity marking (RAM)[36] system. RAM uses a synthetic promoter, $P_{RAM}$, derived from multiple immediate early gene (IEG) elements (Fig. 8). Upon IEG induction, the tetracycline transactivation (tTA) protein element is expressed. Expression of the effector gene is sensitive to doxycycline, a tetracycline analog that sequesters the tTA protein. In the absence of doxycycline, the tTA protein binds to the tetracycline response element (TRE) downstream to drive expression of the effector gene. To prove that RAM can be used to label partner-specific neurons, we coinjected AAV2/8-RAM-mKate and AAV1-hSyn-GFP into the female prairie vole medial amygdala (Fig. 9A). Injected animals were taken off doxycycline and given an opposite sex vole to interact with for 24 hours, after which they were sac'd. Animals that received the opposite sex vole showed robust mKate expression, whereas control animals exhibited no mKate labeling (Fig. 9B), suggesting that mKate-labeled neurons in the experimental animals were partner-specific. To confer temporal specificity to eGFP-RPL10a expression, I obtained and packaged a RAM construct that drives expression of Cre recombinase upon IEG induction in the absence of doxycycline. By optimizing when the animals are taken off doxycycline-containing chow, we

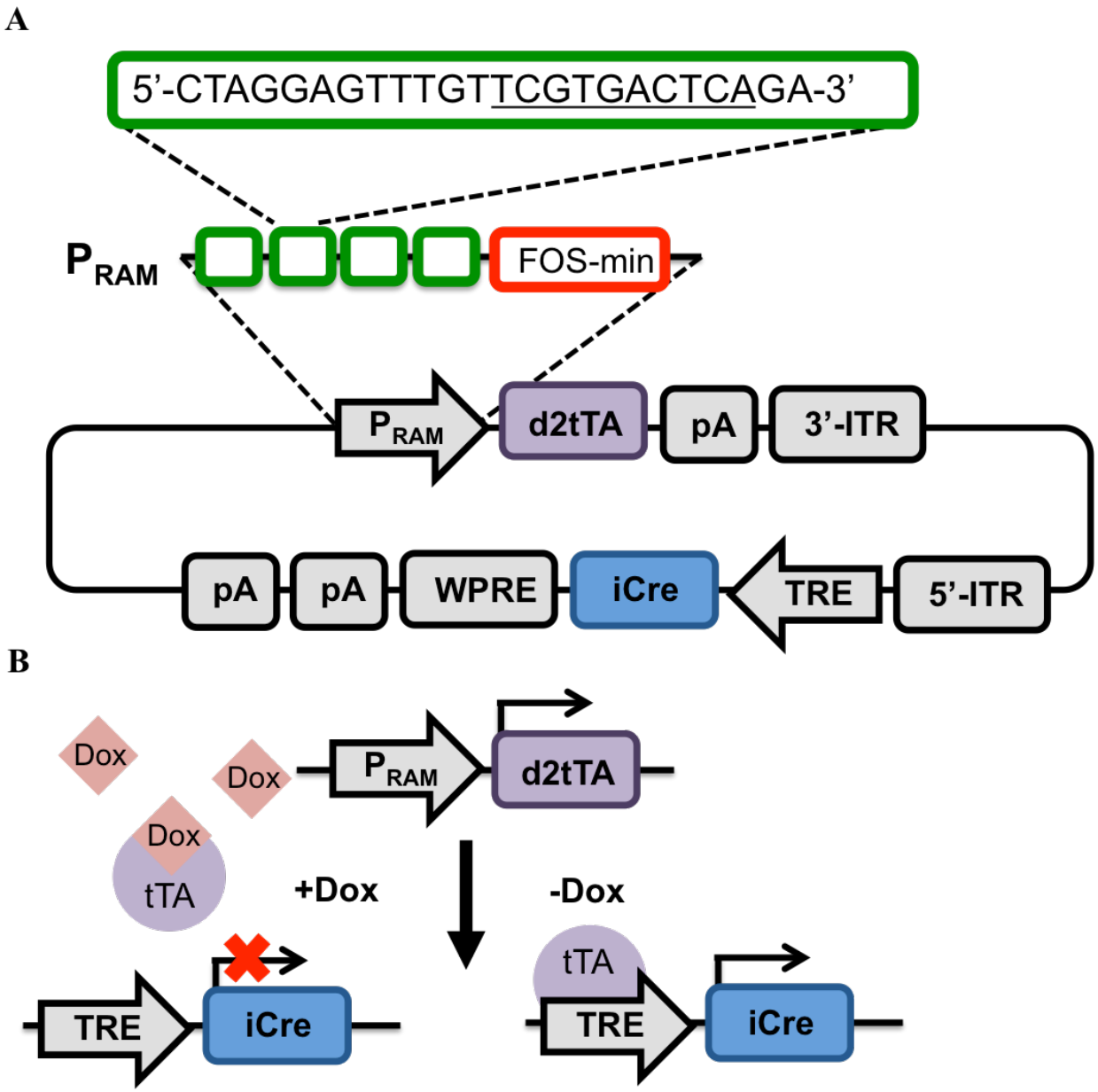


**Figure 8.** The robust activity marking system (RAM) confers temporal control over the expression of Cre recombinase. A) RAM uses a synthetic promoter derived from multiple immediate early gene (IEG) elements. Upon IEG induction, the tetracycline transactivation (tTA) protein element is expressed, and the resulting tTA protein binds to the tetracycline response element (TRE) downstream to drive expression of Cre recombinase (iCre). B) Expression of iCre recombinase is sensitive to doxycycline, a tetracycline analog that is introduced to the animals with doxycycline-containing (DOX) chow. Doxycycline prevents the tTA protein from binding the TRE, preventing expression of Cre recombinase. Image adapted from Sørensen *et al*., 2016.

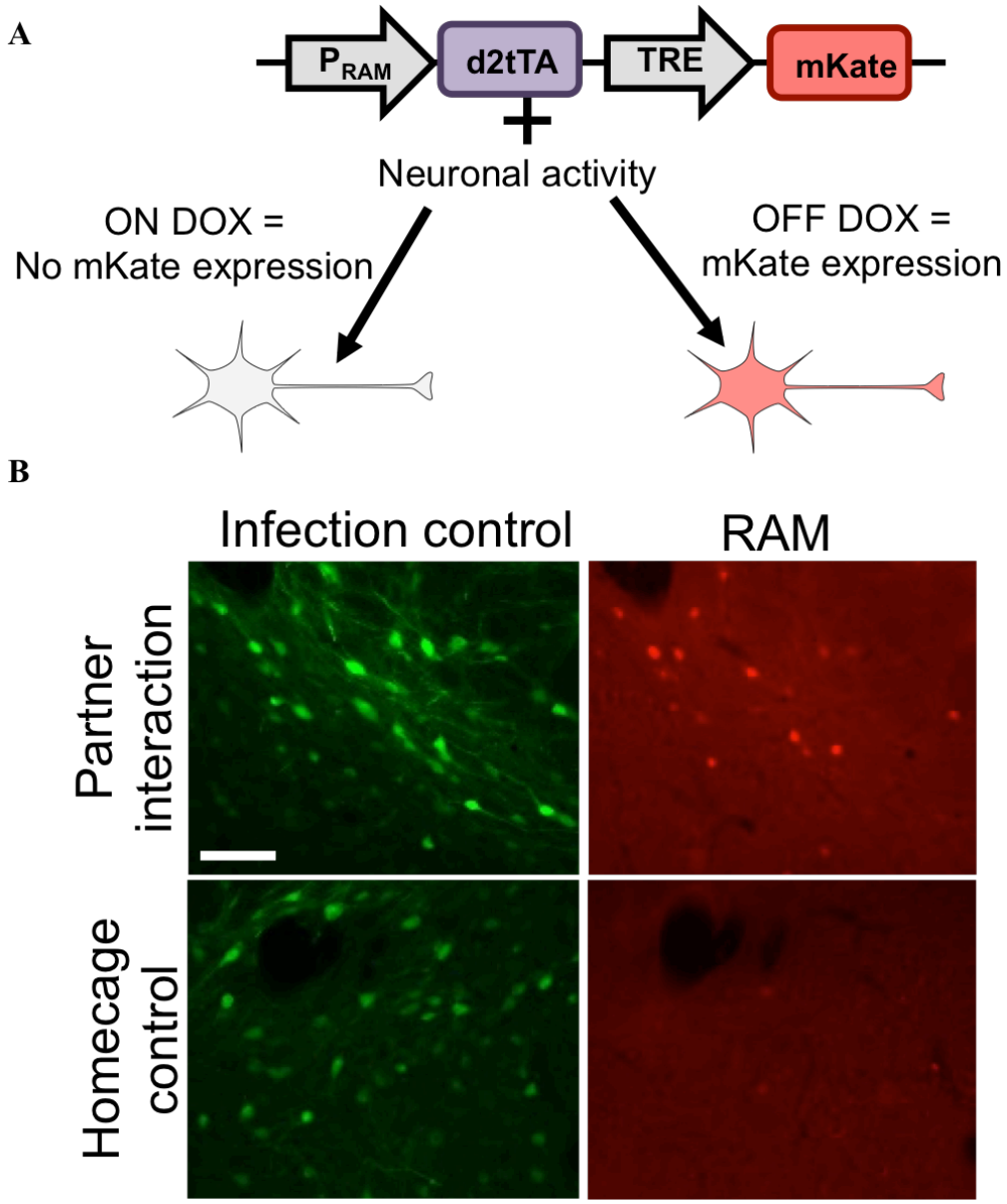


**Figure 9**. Using RAM to label and manipulate active neuronal populations in prairie voles. A) RAM-labeling of active neurons. In the presence of the tetracycline analogue, doxycycline (DOX), tTA cannot bind the TRE. tTA will be expressed in an activity-dependent fashion and, in the absence of doxycycline, will drive expression of the fluorescent reporter mKate. Reapplication of DOX will close the labeling window. B) Proof of efficacy: RAM-labeled cells in prairie vole medial amygdala in response to partner introduction. AAV2/8-RAM-mKate and AAV1-hSyn-GFP were co-injected into the female prairie vole medial amygdala and animals were maintained on DOX chow. 7 days later, animals were switched to regular chow, and 36 hours later, an opposite sex vole was placed in their cage. Brains were collected 24 hours later. Homecage controls had their cage lid removed and the experimenter placed a hand in the cage. Green = infection control. Red = cells activated by partner interaction and labeled with the red fluorophore mKate.

can indelibly express eGFP-RPL10a in neuronal ensembles active during a specific behavioral paradigm such as mating (Fig. 10). The transcriptional profile of neurons active in response to mating can then be characterized, providing evidence for the first time of the global changes in transcription that accompany pair bond formation.

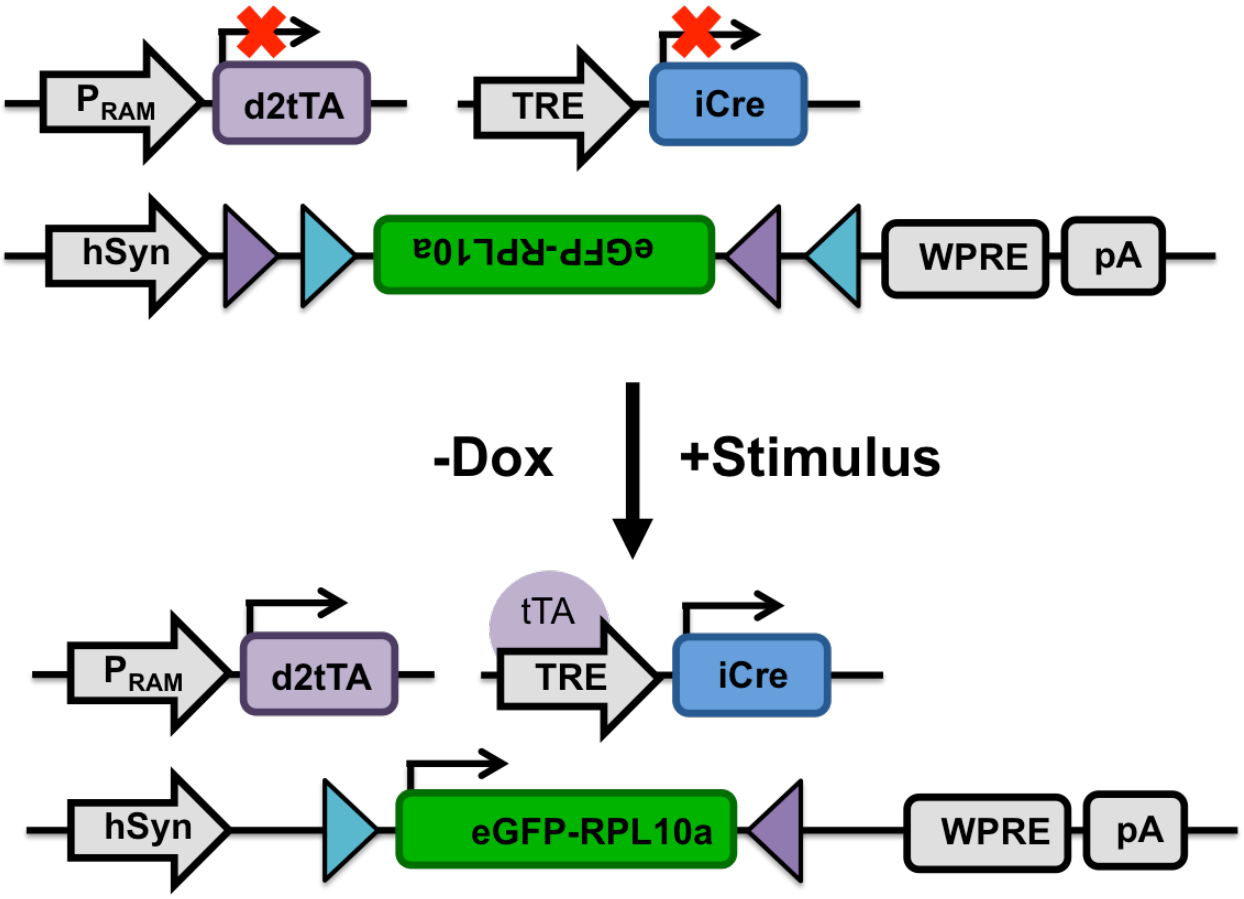


**Figure 10**. The TRAP/RAM-iCre system allows for the isolation of actively translating mRNA of behavior-active neuronal ensembles. In the absence of IEG induction, $P_{RAM}$ is inactive, and neither Cre recombinase nor eGFP-RPL10a are transcribed. Upon cFos induction and in the absence of doxycycline, Cre recombinase is expressed, and the eGFP-RPL10a sequence is inverted into an active orientation. The eGFP-RPL10a mRNA is translated, and the resulting fusion protein is incorporated into the ribosomes of neurons active during a time frame specified by the researcher.

## Supplementary Figures

GGATCACTCTCGGCATGGACGAGCTGTACAAGTCCGGCCGGACTCAGATCTCGAGCTCAAGCTTCGAATTCTTT
GAGCGCAAGCGCAGATCGCTGTCTTCTCTTCCGGTTCCCGCAGCCTCTCCAGCCAGCAGCAAAGTCTCTCGCGA
CACCCTGTACGAGGCGGTGCGGGAGGTCCTGCACGGGAACCAGCGCAAGCGCCGCAAGTTTCTGGAAACGGTGG
AGCTGCAGATCAGCCTGAAGAACTACGACCCCCAGAAGGACAAGCGTTTCTCGGGCACCGTCAGGCTCAAGTCC
ACCCCTCGCCCCAAGTTCTCAGTGTGTGTCCTGGGGGACCAGCAGCACTGCGATGAGGCCAAGGCCGTGGATAT
CCCCCACATGGACATCGAGGCGCTGAAGAAGCTCAATAAGAACAAGAAGTTGGTCAAAAAGCTGGCCAAGAAGT
ATGACGCCTTTCTGGCCTCTGAGTCTCTGATCAAGCAGATCCCGCGTATCCTGGGCCCAGGCCTGAACAAGGCT
GGCAAGTTCCCTTCCCTGCTGACACACAATGAAAACATGGTGGCCAAAGTGGACGAGGTGAAGTCCACGATCAA
GTTCCAGATGAAGAAGGTGCTGTGTCTGGCTGTCGCTGTCGGCCACGTGAAGATGACCGACGACGAGCTGGTCT
ACAACATCCACTTGGCTGTCAATTTCTTGGTGTCCTTGCTCAAGAAGAACTGGCAAAATGTCCGGGCTTTGTAT
ATCAAGAGCACCATGGGCAAGCCCCAGCGTCTTTACTAGGATGCCCCAATAAACCTTCGTGCTACTCTACCATA
ACTTCGTATAATGTA

**Supplementary Figure 1**. RPL10a fragment designed for cloning by Gibson assembly. The sequence is listed 5' to 3'. The sequence consists of a 5' homology arm sequence (blue), a sequence for a protein linker (green), the RPL10a sequence (black, GenBank XM_005360358.1), and a 3' homology arm sequence (purple).

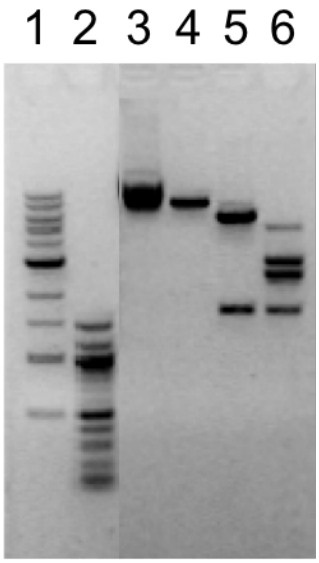


**Supplementary Figure 2**. Restriction digest of pAAV-hSyn-DIO-eGFPpvRPL10a to verify successful cloning. Lane 1: 1kb ladder (NEB). Lane 2: 100bp ladder (NEB). Lane 3: pAAV-hSyn-DIO-eGFPpvRPL10a. Lane 4: pAAV-hSyn-DIO-eGFPpvRPL10a cut with Asc1 (NEB). Lane 5: pAAV-hSyn-DIO-eGFPpvRPL10a cut with Xho1 (NEB). Lane 6: pAAV-hSyn-DIO-eGFPpvRPL10a cut with Asc1 and Xho1.

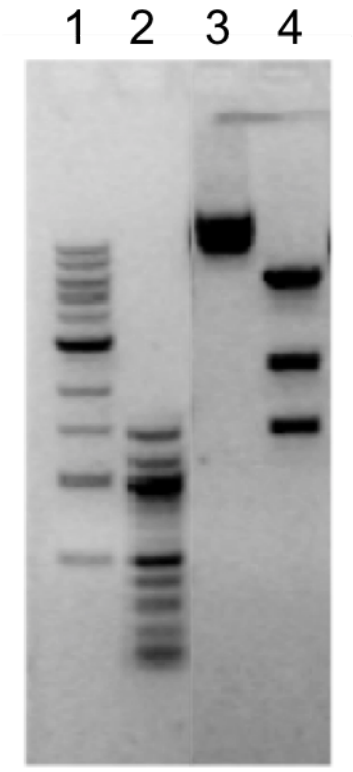


**Supplementary Figure 3**. Restriction digest of pAAV-RAM-d2tTA-TRE-iCre to verify purity and integrity. Lane 1: 1kb ladder (NEB). Lane 2: 100bp ladder (NEB). Lane 3: pAAV-RAM-d2tTA-TRE-iCre. Lane 4: pAAV-RAM-d2tTA-TRE-iCre + Xho1 (NEB).

| Primer Sequence | Notes |
|---|---|
| 5'-AGTTGGGAAGACAACCTGTAGG-3' | |
| 5'-AGAGTTTTCGCCCCGAAGAAC-3' | |
| 5'-CATGGTCCTGCTGGAGTTCGTG-3' | QuintaraBio, QB0020 |
| 5'-CCAGCTTGGTTCCCAATAGA-3' | QuintaraBio, QB0036 |
| 5'-ATAATACCGCGCCACATAGC-3' | QuintaraBio, QB0005 |
| 5'-CGGCATCAGAGCAGATTGTA-3' | QuintaraBio, QB0092 |
| 5'-CATAGCGTAAAAGGAGCAACA-3' | QuintaraBio, QB0112 |
| 5'-GTGTAGGTCGTTCGCTCCA-3' | QuintaraBio, QB0766 |
| 5'-TACGTCTCCGAACTCACGACCG-3' | |
| 5'-TCTTCCTGACTTCATCAGAGG-3' | |
| 5'-TGACAATTCCGTGGTGTTGTCGG-3' | |
| 5'-CAAATGTGGTATGGCTGATT-3' | QuintaraBio, QB0410 |
| 5'-AGCTCGTTTAGTGAACCGTCAGATC-3' | QuintaraBio, QB0043 |
| 5'-AGCGAGTCAGTGAGCGAG-3' | QuintaraBio, QB0039 |
| 5'-TAGAAGGCACAGTCGAGG-3' | QuintaraBio, QB0008 |
| 5'-CTAGCAAAATAGGCTGTCCC-3' | QuintaraBio, QB0099 |
| 5'-TCGAGGTCGACGGTATC-3' | QuintaraBio, QB0070 |

**Supplementary Table 1**. Primers used for sequence verification of pAAV-hSyn-DIO-eGFPpvRPL10a and pAAV-RAM-d2tTA-TRE-iCre.

## References


1. Kikusui, T., Winslow, J. T. & Mori, Y. Social buffering: relief from stress and anxiety. *Philos Trans R Soc Lond B Biol Sci* **361,** 2215–2228 (2006).
2. Yang, Y. C. *et al.* Social relationships and physiological determinants of longevity across the human life span. *PNAS* **113,** 578–583 (2016).
3. Reblin, M. & Uchino, B. N. Social and emotional support and its implication for health. *Curr Opin Psychiatry* **21,** 201–205 (2008).
4. Southwick, S. M., Vythilingam, M. & Charney, D. S. The psychobiology of depression and resilience to stress: implications for prevention and treatment. *Annu Rev Clin Psychol* **1,** 255–291 (2005).
5. Keyes, K. M. *et al.* The Burden of Loss: Unexpected death of a loved one and psychiatric disorders across the life course in a national study. *Am J Psychiatry* **171,** 864–871 (2014).
6. Stroebe, W., Abakoumkin, G. & Stroebe, M. Beyond depression: yearning for the loss of a loved one. *Omega (Westport)* **61,** 85–101 (2010).
7. Shear, M. K. *et al.* Complicated grief and related bereavement issues for DSM-5. *Depress Anxiety* **28,** 103–117 (2011).
8. Kleiman, D. G. Monogamy in Mammals. *The Quarterly Review of Biology* **52,** 39–69 (1977).
9. Sue Carter, C., Courtney Devries, A. & Getz, L. L. Physiological substrates of mammalian monogamy: The prairie vole model. *Neuroscience & Biobehavioral Reviews* **19,** 303–314 (1995).

10. Getz, L. L., Carter, C. S. & Gavish, L. The mating system of the prairie vole, Microtus ochrogaster: Field and laboratory evidence for pair-bonding. *Behav Ecol Sociobiol* **8,** 189–194 (1981).
11. Williams, J. R., Catania, K. C. & Carter, C. S. Development of partner preferences in female prairie voles (Microtus ochrogaster): the role of social and sexual experience. *Horm Behav* **26,** 339–349 (1992).
12. Gruder-Adams, S. & Getz, L. L. Comparison of the Mating System and Paternal Behavior in Microtus ochrogaster and M. pennsylvanicus. *Journal of Mammalogy* **66,** 165–167 (1985).
13. Thomas, J. A. & Birney, E. C. Parental Care and Mating System of the Prairie Vole, Microtus ochrogaster. *Behavioral Ecology and Sociobiology* **5,** 171–186 (1979).
14. Insel, T. R., Preston, S. & Winslow, J. T. Mating in the monogamous male: behavioral consequences. *Physiol. Behav.* **57,** 615–627 (1995).
15. Getz, L. L. & Carter, C. S. Prairie-vole partnerships. *American Scientist; Research Triangle Park* **84,** 56 (1996).
16. Gobrogge, K. & Wang, Z. The ties that bond: neurochemistry of attachment in voles. *Current Opinion in Neurobiology* **38,** 80–88 (2016).
17. Wilson, S. C. Parent-Young Contact in Prairie and Meadow Voles. *Journal of Mammalogy* **63,** 300–305 (1982).
18. Insel, T. R. & Shapiro, L. E. Oxytocin receptor distribution reflects social organization in monogamous and polygamous voles. *Proc Natl Acad Sci U S A* **89,** 5981–5985 (1992).
19. Insel, T. R., Wang, Z. X. & Ferris, C. F. Patterns of brain vasopressin receptor distribution associated with social organization in microtine rodents. *J. Neurosci.* **14,** 5381–5392 (1994).

20. Insel, T. R. & Hulihan, T. J. A gender-specific mechanism for pair bonding: oxytocin and partner preference formation in monogamous voles. *Behav. Neurosci.* **109,** 782–789 (1995).
21. Young, L. J., Nilsen, R., Waymire, K. G., MacGregor, G. R. & Insel, T. R. Increased affiliative response to vasopressin in mice expressing the V1a receptor from a monogamous vole. *Nature* **400,** 766–768 (1999).
22. Lim, M. M. *et al.* Enhanced partner preference in a promiscuous species by manipulating the expression of a single gene. *Nature* **429,** 754–757 (2004).
23. Liu, Y. & Wang, Z. X. Nucleus accumbens oxytocin and dopamine interact to regulate pair bond formation in female prairie voles. *Neuroscience* **121,** 537–544 (2003).
24. Aragona, B. J., Liu, Y., Curtis, J. T., Stephan, F. K. & Wang, Z. A critical role for nucleus accumbens dopamine in partner-preference formation in male prairie voles. *J. Neurosci.* **23,** 3483–3490 (2003).
25. Resendez, S. L. & Aragona, B. J. Aversive motivation and the maintenance of monogamous pair bonding. *Reviews in the Neurosciences* **24,** 51–60 (2012).
26. Resendez, S. L. *et al.* Dopamine and opioid systems interact within the nucleus accumbens to maintain monogamous pair bonds. *eLife Sciences* **5,** e15325 (2016).
27. Aragona, B. J. *et al.* Nucleus accumbens dopamine differentially mediates the formation and maintenance of monogamous pair bonds. *Nature Neuroscience* **9,** 133 (2005).
28. Gobrogge, K. L., Liu, Y., Young, L. J. & Wang, Z. Anterior hypothalamic vasopressin regulates pair-bonding and drug-induced aggression in a monogamous rodent. *PNAS* **106,** 19144–19149 (2009).
29. Heiman, M. *et al.* A translational profiling approach for the molecular characterization of CNS cell types. *Cell* **135,** 738–748 (2008).

30. Heiman, M., Kulicke, R., Fenster, R. J., Greengard, P. & Heintz, N. Cell-Type-Specific mRNA Purification by Translating Ribosome Affinity Purification (TRAP). *Nat Protoc* **9,** 1282–1291 (2014).
31. Preibisch, S., Saalfeld, S. & Tomancak, P. Globally optimal stitching of tiled 3D microscopic image acquisitions. *Bioinformatics* **25,** 1463–1465 (2009).
32. Rubio, J., Li, X., Liu, Q., Cimbro, R., & Hope B. Fluorescence Activated Cell Sorting (FACS) and Gene Expression Analysis of Fos-expressing Neurons from Fresh and Frozen Rat Brain Tissue. *J. Vis. Exp*. **114** (2016).
33. Zhang, Z., Schwartz, S., Wagner, L. & Miller, W. A Greedy Algorithm for Aligning DNA Sequences. *Journal of Computational Biology* **7,** 203–214 (2000).
34. Shapiro, E., Biezuner, T. & Linnarsson, S. Single-cell sequencing-based technologies will revolutionize whole-organism science. *Nature Reviews Genetics* **14,** 618–630 (2013).
35. Yuste, R. From the neuron doctrine to neural networks. *Nature Reviews Neuroscience* **16,** 487 (2015).
36. Sørensen, A. T. *et al.* A robust activity marking system for exploring active neuronal ensembles. *eLife* **5** (2016).
37. Kügler, S., Kilic, E. & Bähr, M. Human synapsin 1 gene promoter confers highly neuron-specific long-term transgene expression from an adenoviral vector in the adult rat brain depending on the transduced area. *Gene Ther* **10,** 337–347 (2003).

## Acknowledgments

The time I have spent in Dr. Zoe Donaldson's laboratory has been invaluable. Over the past one and a half years, she has provided me with the professional resources and knowledge I needed to succeed as an up-and-coming scientist. She inspires me not only as a professional mentor but also an individual, treating my many mistakes with kindness and humor. More importantly, Dr. Donaldson has helped me realize my identity as a scientist, and I hope to carry on her spirit of inclusiveness wherever I go next.

In addition, I would like to thank everyone in the Donaldson lab for the support and friendship they provided. Julie Sadino was instrumental in the realization of this project, as she provided training and feedback at nearly every step. I would also like to thank PRAs Katelyn Gordon and Ashley Cunningham not only for training me but also for providing me with the emotional and intellectual support I needed to thrive. Without everyone in the Donaldson lab family, this project would never have come to fruition.

I am also grateful for the department of Molecular, Cellular, & Developmental Biology for challenging me intellectually and providing me with the resources necessary to ensure my success.

This project was supported by the Undergraduate Research Opportunity Program (UROP) and Biological Science Initiative (BSI). Without the support of these programs, I would never have been able to dedicate enough time to my research.